Submitted to The Astrophysical Journal
Preprint typeset using LaTeX style emulateapj v. 6/22/04

THE X-RAY CONCENTRATION-VIRIAL MASS RELATION

David A. Buote[1], Fabio Gastaldello[1], Philip J. Humphrey[1], Luca Zappacosta[1], James S. Bullock[1], Fabrizio Brighenti[2,3], & William G. Mathews[2]

Submitted to The Astrophysical Journal

ABSTRACT

We present the concentration (c)-virial mass (M) relation of 39 galaxy systems ranging in mass from individual early-type galaxies up to the most massive galaxy clusters, $(0.06-20)\times10^{14}M_{\odot}$. We selected for analysis the most relaxed systems possessing the highest quality data currently available in the *Chandra* and *XMM* public data archives. A power-law model fitted to the X-ray $c-M$ relation requires at high significance (6.6σ) that c decreases with increasing M, which is a general feature of CDM models. The median and scatter of the $c-M$ relation produced by the flat, concordance ΛCDM model ($\Omega_{\rm m}=0.3$, $\sigma_8=0.9$) agrees with the X-ray data provided the sample is comprised of the most relaxed, early forming systems, which is consistent with our selection criteria. Within the context of the concordance model the $c-M$ relation requires $0.76<\sigma_8<1.07$ (99% conf.). The tilted, low-σ_8 model suggested by a new WMAP analysis is rejected at $>99.99\%$ confidence, but it can be reconciled with the X-ray data by increasing the dark energy equation of state parameter to $w\approx-0.8$. When imposing the additional constraint of the tight relation between σ_8 and $\Omega_{\rm m}$ from studies of cluster abundances, the X-ray $c-M$ relation excludes ($>99\%$ conf.) both open CDM models and flat CDM models with $\Omega_{\rm m}\approx1$. This result provides novel evidence for a flat, low-$\Omega_{\rm m}$ universe with dark energy using observations only in the local ($z\ll1$) universe. Possible systematic errors in the X-ray mass measurements of a magnitude $\approx10\%$ suggested by CDM simulations do not change our conclusions.

Subject headings: X-rays: galaxies: clusters — X-rays: galaxies — dark matter — cosmological parameters — cosmology: observations

1. INTRODUCTION

The current cosmological paradigm of a flat universe with low matter density ($\Omega_{\rm m}$) consisting of Cold Dark Matter (CDM) and dark energy has become established recently through a variety of astronomical observations, especially the Cosmic Microwave Background (CMB), supernova Hubble diagram, and statistics of large galaxy surveys (e.g., Spergel et al. 2003; Astier et al. 2006; Spergel et al. 2006). These key techniques probe the large-scale, high-redshift universe where the development of cosmic structure may be studied in the linear clustering regime ($\delta\ll1$). Although the standard model appears to have withstood every test thus far (e.g., Primack 2006), testing the ΛCDM model on small scales, fully into the non-linear regime ($\delta\gg1$), will further our understanding of galaxy formation and evolution and may also refine the fundamental parameters of the world model itself.

The dark matter halos of galaxies and clusters are the largest virialized manifestations of small-scale, non-linear clustering. An important probe of the structure of dark matter halos is the relationship between concentration and virial mass. The concentration parameter is defined as, $c\equiv r_{\Delta}/r_s$, where r_{Δ} – the "virial radius" – is usually taken to be the radius within which the average density equals $\Delta\rho_c$, where ρ_c is the critical density of the universe, and Δ is a number typically between $100-500$. The quantity r_s is the scale radius of the NFW profile (Navarro et al. 1997), but it is replaced by r_{-2}, the radius where the logarithmic density slope equals -2, for more general profiles (Navarro et al. 2004; Graham et al. 2006). The virial mass (M) is the mass enclosed within r_{Δ}.

N-body simulations of CDM models find that c declines slowly with increasing M but with substantial intrinsic scatter, independent of M (Bullock et al. 2001, hereafter B01; Dolag et al. 2004, hereafter D04; Kuhlen et al. 2005; Shaw et al. 2006; Macciò et al. 2006). For a given M the value of c in CDM models varies significantly with changes in cosmological parameters, particularly the normalization σ_8 and w, the parameter representing the dark energy equation of state (Eke et al. 2001; Alam et al. 2002; D04; Kuhlen et al. 2005). The amount of intrinsic scatter in the $c-M$ relation is a robust prediction of CDM models, though preferentially selecting relaxed, early forming systems yields smaller scatter than for the entire halo population (Jing 2000; Wechsler et al. 2002; Macciò et al. 2006).

The expected decrease of c with increasing M in CDM models has yet to be confirmed by observations. Optical studies of groups and clusters ($M>10^{13}M_{\odot}$) using several different techniques – galaxy dynamics (Biviano & Salucci 2006; Łokas et al. 2006), redshift-space caustics (Rines & Diaferio 2006), and weak gravitational lensing (Mandelbaum et al. 2006) – all are consistent with no variation in c. However, the $c-M$ relations obtained by these studies are consistent with the concordance ΛCDM model.

X-ray studies of the $c-M$ relation using data from the *ASCA* satellite (Wu & Xue 2000; Sato et al. 2000) found, $c\sim M_{200}^{-0.5}$, much steeper than produced in CDM models (B01; D04; Macciò et al. 2006). However, it has

[1] Department of Physics and Astronomy, University of California at Irvine, 4129 Frederick Reines Hall, Irvine, CA 92697-4575
[2] UCO/Lick Observatory, Board of Studies in Astronomy and Astrophysics, University of California, Santa Cruz, CA 95064
[3] Dipartimento di Astronomia, Università di Bologna, via Ranzani 1, Bologna 40127, Italy

only become possible with data from the *Chandra* and *XMM* satellites to obtain spatially resolved temperature measurements of sufficient quality for reliable X-ray constraints on the mass profiles of elliptical galaxies, galaxy groups, and clusters (e.g., see reviews by Buote 2004; Arnaud 2005, and references therein). Indeed, our recent study of the mass profiles of seven early-type galaxies with *Chandra* indicates $c-M$ values consistent with ΛCDM. The $c-M$ relations for clusters ($M > 10^{14} M_\odot$) obtained using *XMM* (Pointecouteau et al. 2005) and *Chandra* (Vikhlinin et al. 2006) each are consistent with no variation in c and with the gentle decline with increasing M expected for CDM models. In each case the scatter in $\log_{10} c$ about the mean relation is not well constrained and is consistent with the CDM prediction.

Our present investigation aims to improve significantly the constraints on the $c-M$ relation by analyzing a wider mass range with many more systems than the previous *Chandra* and *XMM* studies. For this purpose we undertook a program to obtain accurate mass constraints on relaxed systems with $10^{12} \lesssim M \lesssim 10^{14} M_\odot$, representing 24 individual early-type galaxies and galaxy groups/clusters, each of which possesses high-quality *Chandra* and/or *XMM* data (Humphrey et al. 2006; Gastaldello et al. 2006; Zappacosta et al. 2006). To these systems we added results for 15 relaxed, massive clusters from Pointecouteau et al. (2005) and Vikhlinin et al. (2006). Using this combined sample, optimized for X-ray mass measurements, we obtain empirical constraints on the local $c-M$ relation with a simple power-law model and compare this model to the predictions of a suite of CDM models.

The paper is organized as follows. We describe the X-ray c and M measurements in §2. Our procedure for fitting a power-law model to the $c-M$ data is discussed in §3. We define the cosmological models that are compared to the X-ray data in §4. We present our results in §5 and discuss sources of systematic error in §6. In §7 we give our conclusions. All distance-related quantities, unless stated otherwise, are computed assuming a flat universe with $\Omega_{\rm m} = 0.3$, $\Omega_\Lambda = 0.7$, and $H_0 = 100h$ km s^{-1} Mpc^{-1} with $h = 0.7$.

2. OBSERVATIONS

The measurements of concentrations and virial masses of 23 early-type galaxies and galaxy groups (Humphrey et al. 2006; Gastaldello et al. 2006) form the core of our sample. In these papers we considered only those systems with the highest quality *Chandra* and/or *XMM* data. Moreover, to insure that hydrostatic equilibrium is a good approximation, we visually inspected all the early-type galaxies and groups in the public data archives and selected those systems that possessed the most regularly shaped X-ray images devoid of strong asymmetries.

To these we added several clusters to populate the high-mass portion of the $c-M$ diagram. Firstly, we include our analysis of the radio-quiet (and very symmetrical) cluster A2589 (Zappacosta et al. 2006). Secondly, we added clusters from the *XMM* study by Pointecouteau et al. (2005) and the *Chandra* study by Vikhlinin et al. (2006), each of whom also focused on the highest quality observations of the most relaxed systems. For clusters that are common to both studies, we used results from Vikhlinin et al. (2006) because of more accurate background subtraction and temperature constraints, the latter resulting from the much smaller point spread function of *Chandra*; i.e., less biased temperature measurements in the presence of strong temperature gradients. For those few (lowest mass) systems in the Pointecouteau et al. (2005) and Vikhlinin et al. (2006) studies that overlap with our work cited above, we use our values.

The final sample (see Table 1) consists of 39 systems spanning the mass range $(0.06-20)\times10^{14} M_\odot$, with c and M values inferred using the NFW dark matter profile. We follow the convention that defines the virial radius ($r_{\rm vir}$) so that the mean density within $r_{\rm vir}$ equals $\Delta\rho_c$, where $\rho_c(z)$ is the critical density of the universe at redshift z, and Δ is obtained from the solution to the top-hat spherical collapse model. To evaluate Δ we use the approximation obtained by Bryan & Norman (1998). For simplicity, when considering DE models with $w \neq -1$, we adopt the value of Δ appropriate for $w = -1$. Although technically the virial overdensity changes with $w \neq -1$ Kuhlen et al. (2005), this choice has no effect on our conclusions. The values of Δ for the concordance cosmology at the appropriate redshift for each system are listed in Table 1.

For results obtained using Δ values different from those in Table 1, we converted c and M to our adopted Δ using the formula of Hu & Kravtsov (2003), which assumes an NFW mass profile. We converted the standard deviations for c and M in one of two ways. For those systems taken from our previous work, we have at least 20 Monte Carlo error simulations. Hence, we convert each simulated value of c and M to the new Δ and then compute the standard deviation of the converted values. This procedure provides a self-consistent conversion of the standard deviations. For systems taken from the literature, we simply convert the lower limit (e.g., $c-\sigma_c$) and upper limit (e.g., $c+\sigma_c$) each to the new Δ. The new standard deviation is then set to one-half the difference of the converted upper and lower limits. (By performing this procedure on our own data and comparing to the rigorous method using the error simulations, we find that this procedure is adequate for our present study.)

Since we perform our analysis of the $c-M$ relation in log space (see below), we also require the standard deviations of $\log_{10} c$ and $\log_{10} M$. As above, for systems analyzed in our previous studies, we compute self-consistently the log errors using Monte Carlo error simulations. The other systems use the simple prescription noted above, but using the log values. The log errors on c and M are listed in Table 1 as, respectively, $\sigma_{\log c}$ and $\sigma_{\log M}$.

For the systems with Monte Carlo error simulations we also computed the covariance between c and M (and $\log_{10} c$ and $\log_{10} M$) for the different systems; e.g., $\sum(c_i - \langle c\rangle)(M_i - \langle M\rangle)$, where the brackets represent the mean quantity, and the sum is over the simulations. In Table 1 we report these as the correlation coefficient, which is the covariance divided by $\sigma_c\sigma_M$ (or $\sigma_{\log c}\sigma_{\log M}$). For the objects from the literature we used the average covariance obtained from the others to evaluate the correlation coefficient. (The small values of the correlation coefficient, especially for the log values, indicate they have little impact on the results presented below.)

TABLE 1
Halo Concentration and Virial Mass

Name (1)	z (2)	Δ (3)	c_0 (4)	σ_{c_0} (5)	$\sigma_{\log c_0}$ (6)	M ($M_\odot$) (7)	σ_M ($M_\odot$) (8)	$\sigma_{\log M}$ (9)	Corr (10)	$\mathrm{Corr}_{\log}$ (11)	Ref. (12)
NGC4125	0.0045	101.5	10.19	1.78	7.52e-02	6.24e+12	8.04e+11	6.24e-02	-1.78e-02	-2.77e-04	a
NGC720	0.0058	101.6	18.54	7.25	1.65e-01	6.65e+12	1.42e+12	9.63e-02	-6.58e-02	-7.67e-04	a
NGC6482	0.0131	102.3	18.40	5.39	1.35e-01	7.15e+12	1.72e+12	8.63e-02	-5.95e-02	-6.35e-04	a
NGC5129	0.0230	103.1	14.95	2.46	7.71e-02	1.54e+13	2.18e+12	5.96e-02	-2.10e-02	-2.65e-04	b
NGC1407	0.0059	101.7	17.88	4.93	1.09e-01	1.59e+13	3.12e+12	9.35e-02	-4.54e-02	-5.15e-04	a
NGC533	0.0185	102.7	17.32	1.21	3.14e-02	2.29e+13	1.11e+12	2.05e-02	-3.05e-03	-3.54e-05	b
NGC2563	0.0149	102.4	10.16	3.43	1.16e-01	2.61e+13	5.46e+12	9.78e-02	-6.35e-02	-8.17e-04	b
RGH80	0.0379	104.4	10.28	1.01	4.15e-02	2.81e+13	1.60e+12	2.55e-02	-5.14e-03	-7.21e-05	b
NGC1550	0.0124	102.2	17.16	1.12	2.80e-02	3.12e+13	1.49e+12	2.08e-02	-2.96e-03	-3.35e-05	b
NGC4472	0.0033	101.4	13.07	1.64	5.09e-02	3.27e+13	3.99e+12	5.97e-02	-1.36e-02	-1.79e-04	a
NGC4325	0.0257	103.3	11.46	1.28	5.61e-02	3.50e+13	8.10e+12	8.34e-02	-2.50e-02	-3.21e-04	b
NGC4649	0.0037	101.5	20.80	2.45	5.17e-02	3.50e+13	4.62e+12	6.29e-02	-1.38e-02	-1.57e-04	a
NGC5044	0.0090	101.9	11.32	0.29	1.09e-02	3.73e+13	1.17e+12	1.40e-02	-7.69e-04	-1.02e-05	b
IC1860	0.0223	103.1	9.59	0.88	3.91e-02	5.10e+13	4.62e+12	3.98e-02	-8.01e-03	-1.12e-04	b
MKW4	0.0200	102.9	12.72	0.86	2.96e-02	6.22e+13	3.38e+12	2.39e-02	-3.47e-03	-4.40e-05	b
NGC4261	0.0075	101.8	3.72	0.86	1.09e-01	6.69e+13	1.03e+13	6.35e-02	-2.93e-02	-6.96e-04	a
RXJ1159.8+5531	0.0810	108.0	11.48	2.86	1.28e-01	9.10e+13	6.89e+13	1.73e-01	-1.53e-01	-1.47e-03	b
A262	0.0163	102.5	8.87	0.67	3.46e-02	1.11e+14	1.06e+13	3.99e-02	-7.05e-03	-1.02e-04	b
MS0116.3-0115	0.0452	105.0	6.57	2.21	1.41e-01	1.28e+14	8.04e+13	2.14e-01	-1.76e-01	-2.54e-03	b
ESO5520200	0.0314	103.8	7.79	0.75	4.46e-02	1.31e+14	1.96e+13	6.06e-02	-1.38e-02	-2.05e-04	b
MKW9	0.0498	105.4	7.48	0.93	5.41e-02	1.44e+14	3.61e+13	1.11e-01	-2.01e-02	-4.54e-04	d
AWM4	0.0317	103.9	9.27	0.84	3.72e-02	1.62e+14	1.82e+13	5.10e-02	-9.34e-03	-1.29e-04	b
ESO3060170	0.0358	104.2	9.17	1.04	6.12e-02	1.81e+14	7.56e+13	1.09e-01	-4.19e-02	-4.76e-04	b
A2717	0.0490	105.3	6.45	0.36	2.46e-02	1.83e+14	1.20e+13	2.84e-02	-3.55e-03	-5.95e-05	b
A1991	0.0592	106.2	8.91	0.66	3.22e-02	1.93e+14	2.67e+13	6.04e-02	-1.26e-02	-4.13e-04	e
A1983	0.0442	104.9	5.34	0.99	8.15e-02	1.99e+14	7.62e+13	1.76e-01	-2.04e-02	-5.39e-04	d
A2589	0.0414	104.7	6.36	0.32	2.33e-02	3.24e+14	2.37e+13	3.00e-02	-3.53e-03	-5.79e-05	c
A2597	0.0852	108.4	8.26	0.70	3.71e-02	3.56e+14	3.91e+13	4.80e-02	-7.39e-03	-4.21e-04	d
A383	0.1883	116.8	9.61	0.89	4.03e-02	4.70e+14	4.76e+13	4.41e-02	-4.80e-03	-3.89e-04	e
A133	0.0569	106.0	6.72	0.61	3.97e-02	5.37e+14	6.44e+13	5.23e-02	-6.01e-03	-4.60e-04	e
A1068	0.1375	112.7	5.44	0.38	3.07e-02	6.96e+14	6.01e+13	3.76e-02	-5.73e-03	-5.14e-04	d
A907	0.1603	114.5	7.75	0.94	5.27e-02	7.39e+14	5.99e+13	3.53e-02	-3.79e-03	-4.24e-04	e
A1795	0.0622	106.5	6.80	0.38	2.44e-02	1.02e+15	8.78e+13	3.75e-02	-3.14e-03	-4.49e-04	e
PKS0745	0.1028	109.9	7.32	0.57	3.40e-02	1.20e+15	1.44e+14	5.24e-02	-2.48e-03	-4.31e-04	d
A478	0.0881	108.6	7.61	0.58	3.29e-02	1.25e+15	1.65e+14	5.74e-02	-2.27e-03	-4.22e-04	e
A2029	0.0779	107.8	8.47	0.44	2.26e-02	1.27e+15	1.18e+14	4.02e-02	-2.01e-03	-4.00e-04	e
A1413	0.1429	113.1	6.56	0.38	2.52e-02	1.29e+15	1.29e+14	4.37e-02	-2.57e-03	-4.55e-04	e
A2204	0.1523	113.9	6.77	0.55	3.51e-02	1.41e+15	1.55e+14	4.80e-02	-2.27e-03	-4.46e-04	d
A2390	0.2302	120.0	4.13	0.32	3.41e-02	2.13e+15	2.14e+14	4.38e-02	-2.47e-03	-5.95e-04	e

Note. — Col.(1): Cluster name. Col.(2) Redshift. Col.(3) Reference overdensity for virial radius and mass definition. Col.(4) Concentration scaled to redshift zero, $c_0 = (1+z)c$. Col.(5) Standard deviation on c_0. Col.(6) Standard deviation on $\log_{10} c_0$. Col.(7) Virial mass. Col.(8) Standard deviation on M. Col.(9) Standard deviation on $\log_{10} M$. Col.(10) Correlation coefficient for c_0 and M. Col.(11) Correlation coefficient for $\log_{10} c_0$ and $\log_{10} M$. Col.(12) Reference for c and M values: a – Humphrey et al. (2006), b – Gastaldello et al. (2006), c – Zappacosta et al. (2006), d – Pointecouteau et al. (2005), e – Vikhlinin et al. (2006). Note that literature results obtained at different Δ values have been converted to those in column (3) as explained in §2.

Finally, the results listed in Table 1 for the concentration parameter actually refer to the quantity, $c_0 = (1+z)c$, since this quantity is what is fitted in our analysis below. For $c \propto (1+z)^{-1}$, c_0 represents the concentration of a halo evolved to $z = 0$. Note that c_0 is also used when computing the covariance and correlation coefficient.

3. ANALYSIS METHOD

We focus our analysis on a simple power-law representation of the $c - M$ data,

$$c = \frac{c_{14}}{1+z}\left(\frac{M}{M_{14}}\right)^{\alpha}, \qquad (1)$$

where z is the redshift, and both c_{14} and α are constants independent of M. We set the reference mass to, $M_{14} = 10^{14} h^{-1} M_\odot$, which lies close to the midpoint (in log space) of the mass range of our sample. CDM models generally predict that c decreases with increasing M (e.g., B01; D04; Kuhlen et al. 2005; Macciò et al. 2006). A key goal of our study, therefore, is to determine whether $\alpha < 0$. For the most massive systems ($M \gtrsim 3 \times 10^{14} M_\odot$) in CDM models D04 find that c_{14} is much more sensitive to cosmological parameter variations than α (see §4).

To constrain the parameters of eqn. [1] it is necessary to account for the error estimates on both c and

TABLE 2
Cosmological Model Parameters

Name	$\Omega_{\rm m}$	Ω_Λ	$\Omega_B h^2$	h	σ_8	n_s	-w
ΛCDM1	0.30	0.70	0.022	0.7	0.90	1.00	1.0
ΛCDM3	0.26	0.74	0.022	0.7	0.74	0.95	1.0
DECDM	0.30	0.70	0.022	0.7	0.90	1.00	0.6
QCDM	0.30	0.70	0.022	0.7	0.82	1.00	≈ 0.8
OCDM	0.30	0.00	0.022	0.7	0.90	1.00	···

Note. — $\Omega_{\rm m}$ is the energy density parameter for matter in the universe; Ω_Λ is the energy density parameter associated with a cosmological constant or, more generally, dark energy; Ω_B is the energy density parameter of baryons; h is $H_0/100$ km s^{-1} Mpc^{-1}; σ_8 is the rms mass fluctuation within spheres of comoving radius $8h^{-1}$ Mpc. See §4.

M. Consequently, we employ the BCES method (i.e., bivariate correlated errors with intrinsic scatter) described by Akritas & Bershady (1996) to estimate α, c_{14}, and the intrinsic scatter about the best relation. We performed the BCES fitting using software kindly provided by M. Bershady[4]. Since BCES is a linear regression method we transform eqn. [1] to the form, $y = \alpha x + b$, where $x \equiv \log_{10} M$, $y \equiv c_0 = \log_{10}(1+z)c$, and $b \equiv \log_{10}(c_{14}/M_{14}^\alpha)$. The parameter c_{14} is derived from α and b: $c_{14} = 10^b M_{14}^\alpha$. Since the fractional error $\sigma_{\log M}/\log_{10} M$ is typically smaller by more than an order of magnitude of the fractional error, $\sigma_{\log c_0}/\log_{10} c_0$ (see Table 1), we always use $x = \log_{10} M$ as the independent variable. By default we also use the $\mathrm{Corr}_{\log}$ values in Table 1 for the BCES method. However, as noted above, the $\mathrm{Corr}_{\log}$ values are quite small and have negligible impact on the estimated α and c_{14}.

We determine the best estimate of α and c_{14} by performing the BCES method on 10^6 bootstrap resamplings of the data. We take the mean of the bootstrap simulations to be the best estimates and construct error ellipses about these best values. The confidence contour spacings computed from the bootstrap simulations correspond quite closely to the $\Delta\chi^2$ values for two parameters assuming normally distributed errors.

We estimate the intrinsic scatter on the concentration as,

$$\begin{aligned}\left(\sigma_y^2\right)_{\rm int} &= \left(\sigma_y^2\right)_{\rm total} - \left(\sigma_y^2\right)_{\rm stat} \\ &= \frac{1}{N}\sum_{i=1}^{N}\left(y_i - y_i^{model}\right)^2 - \frac{1}{N}\sum_{i=1}^{N}\sigma_{y_i}^2, \end{aligned} \quad (2)$$

where N is the number of data points $(x_i, y_i) = (\log_{10} M_i, \log_{10} c_{0,i})$ corresponding to the entries in Table 1; $y_i^{model} = \alpha x_i + b$, where α and b are the best (mean) estimates from the bootstrap simulations; and $\sigma_{y_i} = \sigma_{\log c_0}$ in Table 1.

4. COSMOLOGICAL MODELS

In Table 2 we define the CDM-based cosmological models to be compared with the observations. ΛCDM1 is the standard concordance model, which essentially reflects the combined constraints from the first year of WMAP CMB observations, the supernovae Hubble diagram, and the large-scale clustering of galaxies (e.g., Spergel et al. 2003). ΛCDM3 effectively updates ΛCDM1 using the third year of WMAP (Spergel et al. 2006). Each of these models assumes a constant dark energy equation of state with $w = -1.0$ (i.e., a cosmological constant). In addition, we consider a dark energy model with $w = -0.6$ (DECDM) and a quintessence model (QCDM) with a Ratra-Peebles potential (Ratra & Peebles 1988; Peebles & Ratra 2003, and references therein) as implemented in D04. The QCDM model has a nearly constant $w(z) \approx -0.8$ (see Fig. 1 of D04) and a lower σ_8. Finally, we include an open model (OCDM) with the same parameters as ΛCDM1 except with $\Omega_\Lambda = 0$.

The median relation between concentration and virial mass as a function of redshift for CDM halos is described well by the semi-analytic model proposed by B01,

$$c(M,z) = K\frac{1+z_c}{1+z}, \quad (3)$$

where K is the normalization constant, z is the redshift of the halo, and z_c is the redshift when the halo "collapsed". This collapse redshift is defined implicitly by the equation,

$$\sigma(FM) = \delta_c(z_c), \quad (4)$$

where δ_c is the equivalent linear overdensity for spherical collapse at z_c, σ is the $z = 0$ linear rms density fluctuation corresponding to a mass FM, and F is a constant. (Note that eqn. [3] is not a power-law, though over small mass ranges – within a factor of 5-10 – the B01 model can be well approximated by one.) The constants F and K must be specified by comparison with numerical simulations.

For halos with $M \lesssim 10^{13} h^{-1} M_\odot$ it is found that $F = 0.01$ and $K \approx 3.5$ provide the best description of the results from N-body simulations, although $F = 0.001$ and $K \approx 3$ is acceptable (B01; Kuhlen et al. 2005; Macciò et al. 2006). Larger box simulations that focus on higher mass ranges clearly prefer $F = 0.001$. One of us (J. Bullock) finds that $F = 0.001$ and $K = 3.1$ matches the $c - M$ results for CDM halos simulated by Tasitsiomi et al. (2004). For simulations of even more massive clusters ($3.1 - 17 \times 10^{14} h^{-1} M_\odot$), D04 find higher concentrations and that $K = 3.5$ is required for the same F. Consequently, when comparing CDM models to the full mass range of the X-ray data in Table 1 we shall consider the $c - M$ relations obtained with the B01 model using $F = 0.001$ with both $K = 3.1$ and $K = 3.5$. (In §6.3 we discuss further the different F and K values obtained by different investigators.)

In the high-mass "cluster" regime D04 find that the $c - M$ relation for CDM models is adequately parameterized by the simple power-law model given by eqn. [1]. We list the power-law parameters obtained by D04 in Table 3 but converted to our definition of virial radius. (D04 use $\Delta = 200\rho_b = 60\rho_c$ for $\Omega_{\rm m} = 0.3$.) That is, initially we compute $c(M)$ using c_{14} and α from D04 (at $z = 0$). Then we convert the resulting c and M values to $\Delta = 101.1$ using the approximation of Hu & Kravtsov (2003). These values are used to compute the slope and c_{14}, which are listed in Table 3. The parameter c_{14} decreases by $\approx 20\%$ while α remains nearly constant under this transformation. For comparison, in Table 3 we also

[4] http://www.astro.wisc.edu/∼mab/archive/stats/stats.html

TABLE 3
Power-Law Approximation for CDM Clusters

Name	α	c_{14}
ΛCDM1	-0.104	7.63
DECDM	-0.094	9.05
QCDM	-0.111	7.39
OCDM	-0.091	11.47
$\Lambda CDM1_B$	-0.142	8.43
$\Lambda CDM3_B$	-0.154	6.04

Note. — Power-law parameters (eqn. 1) for the theoretical relation between concentration and virial mass of high-mass clusters obtained by D04 for the ΛCDM1, DECDM, QCDM, and OCDM models. We converted the results presented in Table 2 of D04 to our definition of the virial radius at $z = 0$ (i.e., $\Delta = 101.1$). The $\Lambda CDM1_B$ and $\Lambda CDM3_B$ models are the same as the ΛCDM1 and ΛCDM3 models, but we computed the power-law parameters using the B01 model with $F = 0.001$ and $K = 3.5$. See §4.

list α and c_{14} computed from the tangent line to the $c - M$ profiles located at $M = M_{14}$ of the ΛCDM1 and ΛCDM3 models obtained using the B01 approach with $F = 0.001$ and $K = 3.5$. These results are listed as $\Lambda CDM1_B$ and $\Lambda CDM3_B$ respectively. (We note that the virial quantities for the X-ray data in Table 1 all refer to the ΛCDM1 cosmology. For consistent comparison, we also use the ΛCDM1 cosmology when converting all the D04 models mentioned above.)

The concentration is sensitive to the formation time and dynamical state of the halo (e.g., Navarro et al. 1997; Eke et al. 2001; Jing 2000; B01; Wechsler et al. 2002; Macciò et al. 2006). For example, Jing (2000) and Macciò et al. (2006) find that their "relaxed" dark halo samples have concentrations that are systematically larger by $\sim 10\%$ compared to the whole population. Wechsler et al. (2002) found that the halo concentration at fixed mass is set almost exclusively by the "formation epoch" of the halo (the time when the mass accretion rate of the halos is slowed below a critical value). Indeed, when Wechsler et al. (2002) focused on halos with no major mergers since $z = 2$ they found $\sim 10\%$ higher concentrations for that population. Therefore, a proper comparison between the theoretical $c - M$ relation with observations requires the observed and simulated halos be selected in a consistent manner. The X-ray data presented in Table 1 represent objects that were selected to be the most relaxed, X-ray–bright, systems. But the theoretical $c - M$ models discussed above (Table 3) were obtained using all available halos in the N-body simulations. Consequently, we consider this source of systematic error in our comparisons of the CDM models with the X-ray data.

Finally, the magnitude of the intrinsic scatter about the median theoretical $c-M$ relation does not vary over a large class of CDM models and is independent of M. The value of $\sigma_{\log c} \approx 0.14$ ($\log \equiv \log_{10}$) obtained by B01 has been found by several independent investigations (Jing 2000; Tasitsiomi et al. 2004; D04; Macciò et al. 2006); note this consistency is observed after accounting for the fact that ln, rather than $\log_{10}$, is used in these other studies. Early forming, relaxed, halos tend to exhibit smaller scatter $\sigma_{\log c} \approx 0.10$ (Jing 2000; Wechsler et al. 2002; Macciò et al. 2006).

5. RESULTS

Possible systematic errors affecting the X-ray mass measurements of our sample of relaxed galaxies and clusters are expected to be small and do not change the conclusions of the analysis presented here (see beginning of §6 and §6.2).

5.1. *All Halos*

When fitting the power-law relation (eqn. 1) to the entire sample we obtain $\alpha = -0.172 \pm 0.026$ and $c_{14} = 9.0 \pm 0.4$ (quoted errors 1σ). The estimated intrinsic scatter in $\log_{10}(1 + z)c$ is 0.102 ± 0.004 (eqn. 2), with a total scatter of 0.12. In Figure 1 we plot the best-fitting model with intrinsic scatter. Inspection of Figure 1 reveals that the power-law with intrinsic scatter is a good approximate representation of the X-ray results, especially for $\log_{10} M > 13.5$. For lower masses the X-ray measurements tend to lie above the best-fitting model, though most are consistent with lying within the 1σ range covered by the intrinsic scatter. Using equation [3] of Tremaine et al. (2002) we compute a reduced χ^2 value of 1.07 (37 dof) for the fit, confirming the visual impression that the power law is a good, but not perfect, representation of the X-ray data.

The slope α is constrained to be negative at the 6.6σ level, demonstrating at high significance that c decreases with increasing M, as expected in CDM models. In Figure 1 we also plot the theoretical $c - M$ relation for the ΛCDM1 model for both $K = 3.1$ and $K = 3.5$ as discussed in §4. For $\log_{10} M > 14$ the $K = 3.5$ model recommended by D04 for clusters lies very close to, but just below, the empirical power-law fit. Allowing for a systematic $\approx 10\%$ increase in concentration for relaxed, early forming halos (Jing 2000; Wechsler et al. 2002; Macciò et al. 2006) lifts the $K = 3.5$ model slightly over the power-law, with a marginal improvement in the agreement between the models. A recent theoretical study (Wang et al. 2006) finds that the higher mass halos experience less of bias associated with relaxation and formation time. In fact, systematically increasing the concentrations of the $K = 3.5$ model by $\approx 7\%$ would provide a closer match to the empirical power-law fit to the X-ray data.

For $\log_{10} M < 14$ the $K = 3.5$ model must quickly transform into the $K = 3.1$ model as M decreases from the cluster to the galaxy/group regime as discussed in §4. But in this mass range the $K = 3.1$ model lies consistently below the power-law model and is similar to the 1σ lower limit on the power-law given by the intrinsic scatter. Increasing the concentrations of the $K = 3.1$ model by $\approx 10\%$ for relaxed halos improves the agreement with the power-law, and has the effect of essentially pushing the $K = 3.1$ model into the $K = 3.5$ model. With this accounting for the systematic bias arising from relaxed, early forming halos the ΛCDM1 model is an equally good representation of the X-ray data for masses $\log_{10} M > 13.5$. For the lowest masses, the ΛCDM1 model still lies below the power-law (within the 1σ intrinsic scatter) and may represent a real discrepancy.

We summarize this qualitative discussion with a quan-

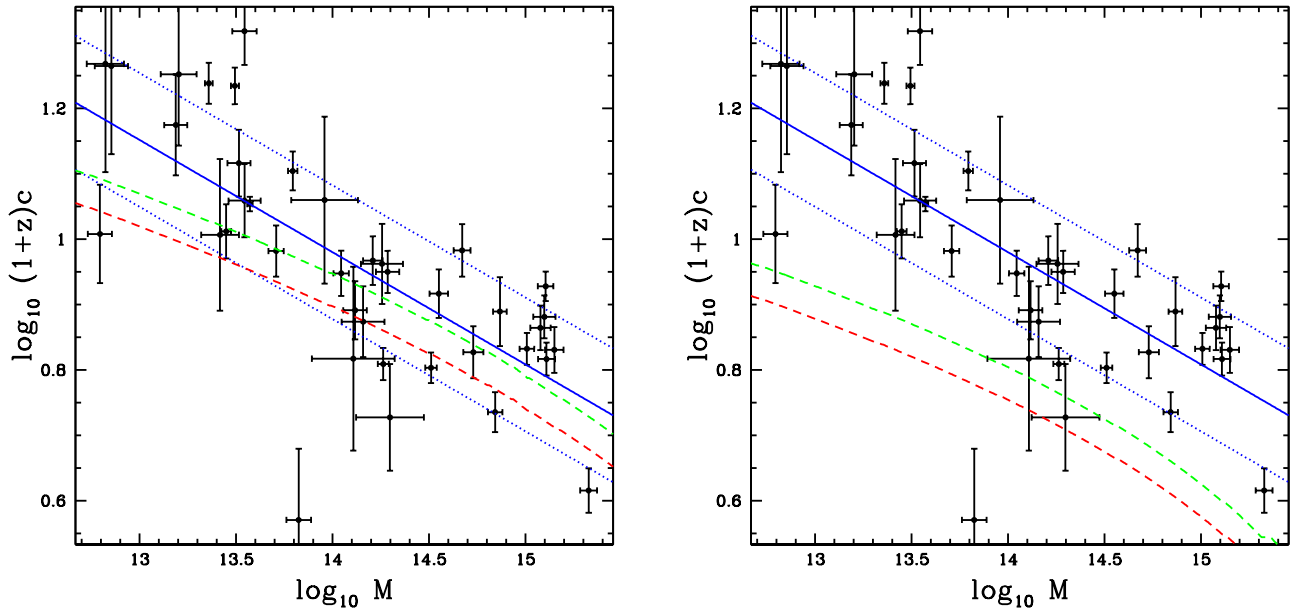

FIG. 1.— Results of fitting eqn. 1 in log space to the entire sample. Displayed are the best-fitting model (solid blue line), the 1σ intrinsic scatter (dotted blue lines), and the predicted relation obtained from cosmological simulations for the (*Left panel*) ΛCDM1 and (*Right panel*) ΛCDM3 models (dashed lines). The two dashed lines attempt to represent fits to different mass ranges in the cosmological simulations as explained in the text (§4). The lower (red) dashed line refers to fits of halos up to $M \sim 0.3 \times 10^{15} M_{\odot}$ ($K = 3.1$) while the upper (green) dashed line refers to fits of higher mass halos $M \approx (0.3 - 1) \times 10^{15} M_{\odot}$ ($K = 3.5$) obtained by D04.

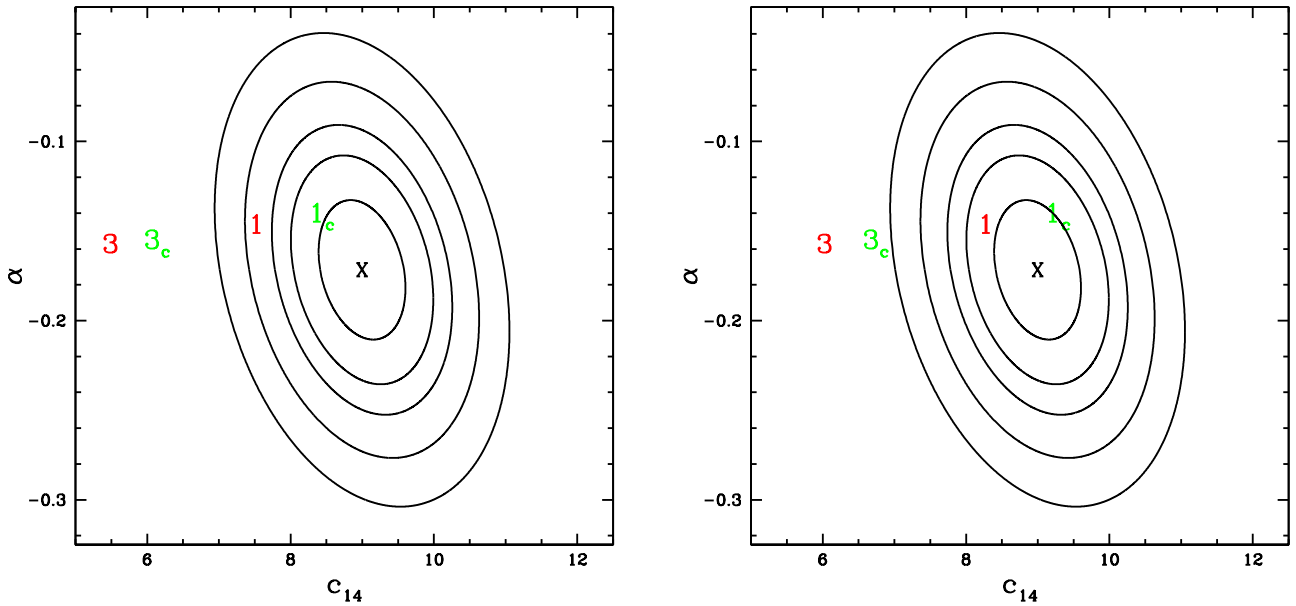

FIG. 2.— Best-fitting value (X) and confidence contours (68%, 95%, 99%, 99.9%, 99.99%) for α and c_{14} obtained from the entire sample. (*Left panel*) As in Fig. 1 results for the ΛCDM1 (green 1) and ΛCDM3 (red 3) models are displayed. Models with subscript "c" refer to the higher normalization $K = 3.5$ for the cluster regime preferred by D04. (*Right panel*) Models have c_{14} increased by 10% to represent relaxed, early-forming halos (see §4 and Macciò et al. 2006).

titative comparison of the ΛCDM1 model with the data as represented by the results of the empirical power-law fit. In Figure 2 we show the error contours estimated for α and c_{14} from the bootstrap simulations (§3). We calculated the slope and concentration of the $c - M$ relation of the ΛCDM1 model at $10^{14} h^{-1} M_{\odot}$ for both the $K = 3.1$ and $K = 3.5$ cases. (The values for $K = 3.5$ are listed in Table 3.) These results are plotted in Figure 2 as "1" for $K = 3.1$ and 1_c for $K = 3.5$, the latter representing the "cluster" regime. The right panel of Figure 2 increases the concentrations by 10% to represent relaxed, early forming systems, and shows the ΛCDM1 model lies near the 68% confidence contour. This level of agreement applies for masses $\log_{10} M > 13.5$. As

discussed above, the agreement is worse at the lowest masses. However, performing a similar comparison at $10^{13}h^{-1}M_{\odot}$ we find the local ΛCDM1 slope and normalization lie just within the 95% confidence contour of the power-law model (both with and without the 10% correction for relaxed systems); i.e., the disagreement is not very significant even at the low-mass end.

The intrinsic scatter of 0.10 in $\log_{10}(1+z)c$ obtained for the power-law fit is smaller than the value of 0.14 for all dark matter halos in CDM simulations but agrees extremely well with the value expected for the most relaxed, early forming systems (Jing 2000; Wechsler et al. 2002; Macciò et al. 2006). Consideration of this result for the scatter and the average $c-M$ relation above, we conclude that the ΛCDM1 model is consistent with the X-ray data, provided the X-ray sample reflects the most relaxed, early forming systems in the population. (This corroborates our selection criteria discussed in §2.)

Now we perform the analogous comparison of the ΛCDM3 model with the X-ray data and associated power-law fit. The $c-M$ relation is displayed in the right panel of Figure 1. The ΛCDM3 model lies well-below the power-law at all masses, even when allowing for the expected 10% increase in concentration for relaxed halos. In Figure 2 we compare the ΛCDM3 model at $10^{14}h^{-1}M_{\odot}$ with the empirical power-law. Even when considering the 10% increase in concentrations for relaxed halos, the ΛCDM3 model lies outside the 99.99% contour. Systematic errors associated with the X-ray measurements cannot explain this level of disagreement (see §6).

The key parameter responsible for the poor performance of the ΛCDM3 model with respect to ΛCDM1 is the low value of σ_8 (0.74). In order to bring the ΛCDM3 model within the 99% contour in the right panel of Figure 2 requires $\sigma_8 > 0.84$ where we have kept the other cosmological parameters fixed to their values in Table 2. This limit is conservative since (1) we use $K = 3.5$, (2) we assume a full 10% upward shift for the bias from relaxed, early forming systems, which may be less for massive clusters, and (3) we have approximated the B01 models as power-laws using their predictions only near $10^{14}h^{-1}M_{\odot}$. The sensitivity of the concentrations to σ_8 results from the impact that σ_8 has on the average halo formation times (e.g., Eke et al. 2001; Alam et al. 2002; van den Bosch et al. 2003).

Other cosmological parameters, however, contribute to the large discrepancy of the ΛCDM3 model. If we remove the tilt of the power spectrum (i.e., set $n_s = 1$) then we obtain $\sigma_8 > 0.80$ at the 99% confidence level. Finally, if we further set $\Omega_{\rm m} = 0.3$ (so the model is the same as ΛCDM1 except with variable σ_8), then the 99% constraint falls to $\sigma_8 > 0.76$, almost consistent with the value of 0.74. (We reiterate this limit is conservative as noted above. Similarly, we obtain $\sigma_8 < 1.07$ at 99% confidence, where the $K = 3.1$ model is used here to be conservative.) Hence, although the lower value of σ_8 is the primary cause of the poor performance of the ΛCDM3 model, the combined action of the power-spectrum tilt with the lower value of $\Omega_{\rm m}$ exacerbate the discrepancy with the X-ray $c-M$ relation.

If the ΛCDM3 parameters are correct, particularly the low value of σ_8, then a fundamental modification of the model is required to increase the concentration values to match the X-ray results. Both D04 and Kuhlen et al. (2005) have shown that changing the dark energy equation of state parameter (w) has the effect of systematically raising (larger w) or lowering (smaller w) halo concentrations. As we show below, a model with $w \approx -0.8$ and $\sigma_8 \approx 0.8$ can describe the X-ray data in the cluster regime.

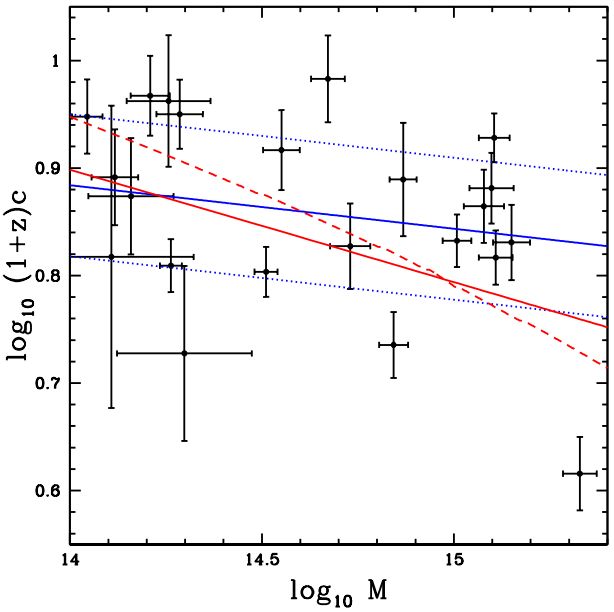

FIG. 3.— Results of fitting eqn. 1 in log space only for halos with $M > 10^{14}M_{\odot}$. Displayed are the best-fitting model (solid blue line) and the 1σ intrinsic scatter (dotted blue lines). Also shown is the predicted relation for the ΛCDM1 model from cosmological simulations. The (solid red) line is the power-law fit obtained by D04 while the (dashed red) line is the B01 model with $F = 0.001$ and $K = 3.5$ found by D04 to best match the simulated clusters. Note the D04 model is converted to our definition of the virial radius (§4).

5.2. *Only Halos with $M > 10^{14}M_{\odot}$*

As discussed in §4, D04 provide results of fitting eqn. [1] to a suite of CDM models for massive clusters, including an open model and multiple dark energy models. We may compare these theoretical predictions directly to the power-law fit to the X-ray data with the following considerations. Firstly, we convert D04's results to our definition of the virial radius (see §4). Secondly, since D04 analyze only massive clusters ($M > 4 \times 10^{14}M_{\odot}$, $h = 0.7$ and converted to $\Delta = 101.1$), we restrict our analysis to high-mass systems as well. In order to allow more precise constraints on the power-law fit we consider clusters down to a somewhat smaller mass limit, $M > 1 \times 10^{14}M_{\odot}$. (As shown below, this choice is justified since there is no obvious trend in the $c-M$ relation over this mass range.) Finally, we need to consider the biases ($\approx 10\%$ higher c, smaller scatter in $\log_{10} c$) for relaxed, early forming systems as done for the whole sample in the previous section. However, the systematic increase in c may be less since we are considering the most massive systems (Wang et al. 2006).

In Figure 3 we show the result of fitting eqn. [1] to the high-mass sample, for which we obtain the following pa-

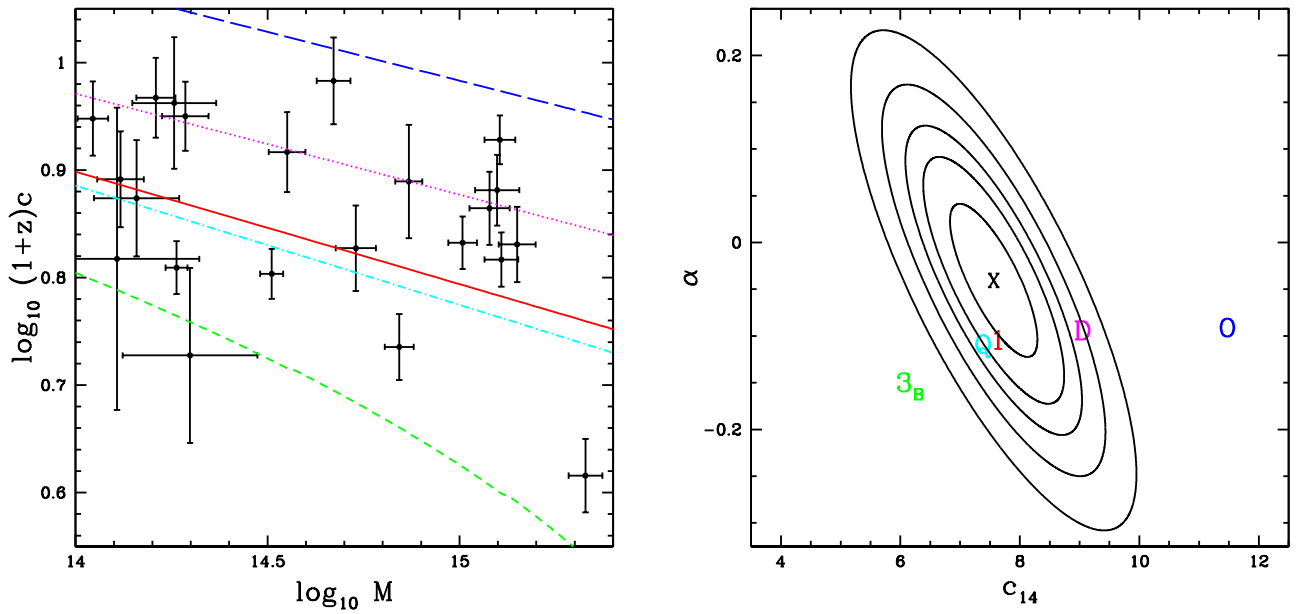

FIG. 4.— (*Left panel*) c-M relations for various CDM models obtained by D04 for galaxy clusters (see Table 3). The solid (red) line is ΛCDM1, the dashed (blue) line is OCDM, the dotted (magenta) line is DECDM, and the dot-dashed (cyan) line is QCDM. Finally, the short dashed (green) line is the ΛCDM3 model computed using the B01 prescription with $K = 3.5$. (*Right panel*) Best-fitting value (X) and confidence contours (68%, 95%, 99%, 99.9%, 99.99%) for α and c_{14} obtained by fitting only systems with $M > 10^{14} M_{\odot}$. Also shown are the results for the models plotted in the left panel: ΛCDM1 (1), OCDM (O), DECDM (D), QCDM (Q), and ΛCDM3 ($3_{\rm B}$).

rameter constraints, $\alpha = -0.04 \pm 0.05$ and $c_{14} = 7.6 \pm 0.5$. These parameters are consistent with a constant $c - M$ relation, as well as profiles that both decrease and increase with increasing M, and agree well with similar fits obtained in this mass range from previous X-ray studies with either *XMM* (Pointecouteau et al. 2005) or *Chandra* (Vikhlinin et al. 2006). Since the power-law fit is quite consistent with $\alpha = 0$, it follows that it is the lower mass systems ($< 10^{14} M_{\odot}$) which require $\alpha < 0$ found when fitting the whole sample in the previous section (see Gastaldello et al. 2006). (Note that the power-law parameters inferred in the previous section for the full sample lies on the 99% confidence contour obtained for the fit to the high-mass subsample – see Figure 4.)

We measure an intrinsic scatter in $\log_{10}\ (1 + z)c$ of 0.07 ± 0.01 which is somewhat less than the value of 0.10 obtained for the entire sample. D04 also obtain 0.10 for the intrinsic scatter (after accounting for a factor of 2.3 converting ln to $\log_{10}$) for all of their CDM clusters. The smaller scatter we measure presumably can be explained because the X-ray sample preferentially contains relaxed, early forming systems.

For comparison we plot two versions of the ΛCDM1 model in Figure 3. The first version we show is the power-law fit obtained by D04 converted to our definition of the virial radius (see §4). The second version arises from using the B01 model with $K = 3.5$, which D04 found to best represent their high-mass cluster simulations. Both models are very similar and provide a reasonable description of the X-ray data, though the B01 representation is slightly steeper.

In the left panel of Figure 4 we plot the power-laws obtained by D04 for the CDM models as well as the B01 representation of the ΛCDM3 model with $K = 3.5$. The values of α and c_{14} for all of these models (Table 3) are plotted in the right panel of Figure 4 along with the error contours derived from the power-law fit to the X-ray data. As done in the previous section, the α and c_{14} values for the B01 ΛCDM3 model were obtained using the $c - M$ slope near $M = 10^{14} h^{-1} M_{\odot}$.

We emphasize that the D04 parameters may be compared directly to the results of our power-law fit to the X-ray data, since the same model is fitted over nearly the same mass range. Since the B01 representation of the ΛCDM3 model is very nearly a power-law over the range being investigated, a similarly direct comparison is appropriate.

The results for the ΛCDM1 and ΛCDM3 models obtained using only the high-mass subsample corroborate those obtained from the full sample. As noted above, the ΛCDM1 model is an acceptable match to the X-ray data; the parameters lie near the 68% confidence contour in Figure 4, even if c is increased to correct for early forming halos. In contrast, the ΛCDM3 model is very inconsistent with the high mass data, with parameters lying outside the 99.99% contour. Even if we apply the full 10% correction to c_{14} appropriate for the most relaxed, early forming systems, then the model merely moves on top of the 99.99% contour. However, as noted above, it is expected that this correction is less for the highest mass systems. Hence, the ΛCDM3 model is also rejected using only the most massive clusters.

The $c - M$ data for high-mass clusters clearly exclude the OCDM model. The concentrations lie systematically above the data and the ΛCDM1 model. The latter is expected because structures form earlier in the OCDM model. In principle, the OCDM model may be brought into acceptable agreement with the X-ray data by lower-

ing σ_8. We estimate the effect of lowering σ_8 using the ΛCDM1 B01 model. For example, lowering σ_8 from 0.90 to 0.70 lowers c_{14} by 25%. This would move the OCDM model to the right in Figure 4 on to the 99% confidence contour. Considering any of the 10% systematic bias expected for early forming systems would increase the discrepancy. (Note that for $\sigma_8 = 0.74$, appropriate for the ΛCDM3 model, the OCDM model would be rejected at the 99.9% confidence level without additional consideration of early formation bias.)

Studies of the abundances of galaxy clusters using weak gravitational lensing typically find σ_8 consistent with 0.9 (e.g., Hoekstra et al. 2002; Van Waerbeke et al. 2005; Jarvis et al. 2003). The optical study of Rines et al. (2006) uses the caustic technique to measure cluster abundances and also finds $\sigma_8 \approx 0.9$ with a lower limit of 0.72 (95% conf.). However, X-ray studies of cluster abundances show a large variation in σ_8, with values ranging from 0.7-0.9 (see Arnaud 2005, and references therein). The X-ray studies use a simple conversion between mass and global temperature or mass and global X-ray luminosity ($L_{\rm x}$). A recent study by Stanek et al. (2006) argues that considering reasonable errors in the $M - L_{\rm x}$ conversion allows agreement of cluster abundances with the recent WMAP parameters with $\sigma_8 = 0.85$ and $\Omega_{\rm m} = 0.24$ – though see Reiprich (2006). We take $\sigma_8 = 0.7$ to be a conservative lower limit established by the abundances of galaxy clusters.

Therefore, an open CDM model with $\Omega_{\rm m} \approx 0.3$ is ruled out (> 99% confidence) from joint consideration of only the X-ray $c - M$ relation and cluster abundances. Since σ_8 and $\Omega_{\rm m}$ are tightly coupled from cluster abundance studies, and all the studies cited above give $\sigma_8 \approx 0.45$ for $\Omega_{\rm m} \approx 1$, using the X-ray $c - M$ data we find that we can also exclude CDM models with $\Omega_{\rm m} \approx 1$ at high significance (> 99.9% confidence). For this comparison we have employed the entire sample of 39 systems and have set $h \approx 0.5$ for the $\Omega_{\rm m} \approx 1$ models to better satisfy cosmic age constraints from stellar populations in globular clusters (Chaboyer 1998). Consequently, the combination of the X-ray $c - M$ relation and cluster abundances, assisted by constraints on the cosmic age, provides novel evidence for a flat, low-$\Omega_{\rm m}$ universe with dark energy using observations only in the local ($z \ll 1$) universe.

Finally, we consider the alternative dark energy models, DECDM and QCDM. The DECDM model lies systematically above the ΛCDM1 model and deviates from the power-law fit to the X-ray data at the 99.9% confidence level. This behavior is expected since $w = -0.6$ implies halos form earlier compared to the $w = -1$ ΛCDM1 model (see also Kuhlen et al. 2005). By lowering σ_8 it should be possible to bring the DECDM model into good agreement with the data. To illustrate this trade-off between w and σ_8, we consider the QCDM model which has $w \approx -0.8$ and $\sigma_8 = 0.82$. As shown in Figure 4 the QCDM model matches the X-ray results nearly as well as the ΛCDM1 model. In fact, a mild increase in c_{14} owing to effect from selecting relaxed, early forming halos would produce even better agreement.

Our analysis indicates that a model similar to QCDM is able to satisfy the most recent constraints from other cosmological observations since $w \approx -0.8$ is marginally consistent with the constraints imposed by supernovas ($w = 1.023 \pm 0.090\,({\rm stat}) \pm 0.054\,({\rm sys})$, Astier et al. 2006), and $\sigma_8 = 0.82$ is also marginally consistent with the 3-yr WMAP results. Put another way, if the low σ_8 value of ΛCDM3 is correct, then the X-ray $c - M$ data imply $-1 < w \approx -0.8$.

6. SYSTEMATIC ERRORS

When comparing to theoretical predictions of the $c-M$ relation we have considered the small biases in the mean concentration level and scatter expected for the highly relaxed, early forming systems selected for our study. We found that the ΛCDM1 model is a good representation of the X-ray data provided this bias for relaxed systems applies, especially for the low-mass range of our sample ($M < 10^{14} M_\odot$). However, the ΛCDM3 model does not agree with the $c - M$ data, even considering this bias.

Could other sources of systematic error seriously affect these conclusions? For 24 of 39 systems in Table 1 we have performed a detailed investigation of systematic errors on c and M (Humphrey et al. 2006; Zappacosta et al. 2006; Gastaldello et al. 2006). Generally, we find that the estimated systematic error is less than the statistical error, particularly for the systems of lowest mass. For the higher mass systems, the errors are usually comparable. But from consideration of all of these systems we recognize no obvious trend that would systematically shift the observed $c - M$ relation in one direction.

Although we do not believe systematic errors associated with the X-ray data analysis compromise the conclusions of our present investigation, here we list the most important issues to be resolved in future studies that seek to use the X-ray $c - M$ relation for precision constraints on cosmological models. Below in §6.2 we also consider the impact on our present analysis of systematic errors resulting from the hydrostatic equilibrium approximation.

(Note we verified that our analysis is insensitive to the definition of the virial radius. An interesting example is to compare to results obtained for $\Delta = 2500$, because within this radius all of the systems in our study possess good X-ray constraints. When defining the virial radius to correspond to $\Delta = 2500$ for every system, we arrive at the same conclusions obtained in §5 but with correspondingly different α and c_{14} values. The predictions of the cosmological models were also converted to $\Delta = 2500$ for this comparison.)

6.1. *Early Formation Bias*

Accounting for the biases associated with preferentially observing the most relaxed, early forming systems is required for precision constraints on cosmology. While Wechsler et al. (2002) found a nearly one-to-one correlation between halo "formation epoch" and concentration, it is not obvious how this theoretically motivated parameter should connect with the dynamical state of a real cluster. More direct quantifiers (e.g. rejecting cases with recent major mergers and disturbed profiles) suggest that "relaxed" halos should have ≈ 10% larger average c and smaller scatter. For massive systems ($M \gtrsim ({\rm few}) \times 10^{14} M_\odot$), the outlook for analyzing a sample with a well-determined, observational selection function is excellent, because there exist several well-defined catalogs of the brightest, most massive clusters in X-rays (e.g., Reiprich & Böhringer 2002), of which many

of the systems have been observed either with *Chandra* or *XMM*. For lower masses the number of X-ray catalogs of complete samples is small, and the number with good coverage with *Chandra* or *XMM* observations is even smaller. For this purpose we have scheduled observations of a complete, X-ray flux-limited sample of 15 systems in the approximate mass range $10^{13} - 10^{14}\,M_\odot$ with *Chandra*.

6.2. *Hydrostatic Equilibrium*

The determination of the mass distribution from X-ray observations requires that hydrostatic equilibrium is a suitable approximation. This approximation has been tested for massive clusters by comparing to results obtained from gravitational lensing (e.g., Buote 2003, and references therein). There is very good agreement between the methods, especially outside the inner cores. This agreement is especially encouraging since some of the clusters are manifestly not completely relaxed (e.g., A2390, Allen et al. 2001). At the low-mass end, good agreement between X-ray mass measurements with stellar dynamics in elliptical galaxies provides further indication that the hydrostatic equilibrium approximation is quite accurate for obviously relaxed systems (Humphrey et al. 2006; Bridges et al. 2006).

For over ten years cosmological hydrodynamical simulations have found that the hydrostatic equilibrium approximation is quite accurate in massive galaxy clusters (e.g., Tsai et al. 1994; Buote & Tsai 1995; Evrard et al. 1996; Mathiesen et al. 1999). The most recent studies conclude that X-ray mass estimates of the most massive, relaxed clusters should typically underestimate the mass by a small amount ($\approx 10\%$) because of turbulent pressure in the hot gas, with less of an effect in lower mass systems (e.g., Dolag et al. 2005; Rasia et al. 2006; Nagai et al. 2006).

The systems analyzed in our present investigation were selected to be highly relaxed – as indicated by regularly shaped X-ray image morphology. This is reinforced by our analysis of the X-ray $c - M$ relation (§5), especially by the small intrinsic scatter in the concentrations which is a robust prediction of CDM models (Jing 2000; Dolag et al. 2004; Wechsler et al. 2002; Macciò et al. 2006).

Underestimating the virial masses of our relaxed clusters by 10%, as suggested by CDM simulations, would indicate that our measurement of c_{14} should be raised by a factor $1.1^{-\alpha} \approx 1.02$, using $\alpha = -0.17$. In addition, since $c \propto (M_{\rm vir})^{1/3}/r_s$, where r_s is the NFW scale radius, the total increase in c_{14} should be $\approx 5\%$, provided the estimate of r_s is unaffected by the presence of turbulent pressure. This systematic error, if real, would have the effect of increasing the discrepancies between the X-ray $c - M$ relation and (most) CDM models. However, essentially all of conclusions in §5 remain unchanged if we consider the bias for relaxed early forming systems to be 15% rather than 10%, within the range obtained by current simulations (Jing 2000; Wechsler et al. 2002; Macciò et al. 2006). The exceptions are the OCDM and DECDM models (§5.2, see Fig. 4), for which the $\approx 5\%$ boost in c_{14} would bring the models into slightly better agreement with the data. However, the OCDM model is still rejected at $> 99.99\%$ confidence, and the $\Omega_{\rm m} \approx 0.3$ open CDM models are still excluded ($> 99\%$ conf.), the latter provided that at least a 5% bias (of the expected $\approx 10\%$) for relaxed, early forming systems applies. We conclude, therefore, that the level of systematic error suggested by CDM simulations to affect the X-ray mass measurements does not change the conclusions of our present study.

6.3. *Semi-Analytic Model Predictions of $c - M$ relation*

In order to use the X-ray $c - M$ relation for precision constraints on cosmological parameters, it is necessary to be able to predict halo concentrations produced in different cosmological models with high precision. This must be achieved with a semi-analytic procedure, because it is not feasible to resort to N-body simulations to fully investigate parameter space for obtaining confidence regions. The procedure proposed by B01 is currently one of the most promising models of this kind. With just two parameters F and K (see §4) it can reproduce the results of CDM N-body simulations with ranges of power spectrum shapes, σ_8 normalizations, matter content, and dark energy variables w (B01, Kuhlen et al. 2005).

Recently, Macciò et al. (2006) show that the normalizations of the B01 models (i.e., K values) obtained by different investigators analyzing halos covering approximately the same mass range ($\lesssim 10^{13} h^{-1} M_\odot$) can differ by 10-20%. For halos with $M \approx 10^{13} - 10^{14} h^{-1} M_\odot$, the halos of Macciò et al. (2006) prefer $F = 0.001$ and $K = 2.6$ while those Tasitsiomi et al. (2004) prefer $K = 3.1$. The "cluster" halos ($\gtrsim 3 \times 10^{14} M_\odot$) studied by D04 suggest a higher normalization $K = 3.5$. Because so few studies have investigated the high-mass halo regime, it is unclear whether these differences reflect numerical details in the simulations or demand a revision of the B01 model. More studies of the concentrations of the highest mass halos are very much needed.

In this context it is important to note that Shaw et al. (2006) have recently studied the $c-M$ relation of massive halos, where most of their halos have $M \approx 1 \times 10^{14} M_\odot$. They obtain power-law fit parameters $\alpha = -0.12 \pm 0.03$ and $c_{14} = 8.30 \pm 0.04$ for the model ΛCDM1 but with $\sigma_8 = 0.95$. Converting their results to $\sigma_8 = 0.90$ yields a 6% reduction in the concentration, $c_{14} = 7.81 \pm 0.04$, which is just 2% larger than the D04 value quoted in Table 3. We consider this quite good agreement, considering the differences between theoretical studies noted above for lower mass halos.

Finally, we mention that if we adopt the lowest normalization quoted in the literature ($F = 0.001$, $K = 2.6$, Macciò et al. 2006) for our entire mass range, then in order for the ΛCDM1 model to match the X-ray data, it is necessary to boost the concentrations produced in the ΛCDM1 model by another 16% over the 10% attributed to the prefential selection of relaxed, early forming systems. This 16% increase can be achieved by increasing either $\sigma_8 (\approx 1.0)$, w (≈ -0.8), or both.

6.4. *Gas Physics & Adiabatic Contraction*

The published CDM predictions for the $c - M$ relation we have considered in this paper are all derived from dissipationless N-body simulations containing only dark matter. While the details of gasdynamics should be unimportant for massive systems ($M \gtrsim 10^{14} M_\odot$), the effects of dissipation and feedback from

star formation and AGN likely influence the dark matter profile inferred from observations of lower mass halos. It is noteworthy that the systems with $M \sim 10^{13} M_{\odot}$ show the largest deviations from the ΛCDM1 model (§5.1). For most of these the *Chandra* data require a significant contribution of stellar mass from the central galaxy (Humphrey et al. 2006; Gastaldello et al. 2006). However, allowing for adiabatic contraction (e.g., Blumenthal et al. 1986; Gnedin et al. 2004) of the dark matter profile in most cases degrades the fits, suggesting a more complex interplay between the baryons and the dark matter (e.g., Loeb & Peebles 2003; El-Zant et al. 2004; Dutton et al. 2006). Future precision cosmology studies which aim to use the X-ray $c - M$ relation for low-mass systems ($M \lesssim 10^{13} M_{\odot}$) will require better understanding of the influence of the central galaxy on the inferred dark matter distribution.

7. CONCLUSIONS

We present the concentration (c)-virial mass (M) relation of 39 galaxy systems ranging in mass from individual early-type galaxies up to the most massive galaxy clusters, $(0.06 - 20) \times 10^{14} M_{\odot}$. We selected for analysis the most relaxed systems possessing the highest quality data currently available in the *Chandra* and *XMM* public data archives. Measurements for 24 systems were taken from our recent work (Humphrey et al. 2006; Gastaldello et al. 2006; Zappacosta et al. 2006) which populate the lower mass portion of the sample ($M \lesssim 10^{14} M_{\odot}$). We obtained results for 15 massive galaxy clusters in our sample from the studies by Pointecouteau et al. (2005) and Vikhlinin et al. (2006).

We parameterize the X-ray $c - M$ relation using a simple power-law model. The best estimates of the parameters – the slope (α) and normalization (c_{14}) evaluated at $M = M_{14} = 10^{14} h^{-1} M_{\odot}$ – were obtained via linear regression in log space taking into account the uncertainties on both c and M. We employed the BCES method of Akritas & Bershady (1996) for this analysis.

Fitting the power-law model to the entire sample yields $\alpha = -0.172 \pm 0.026$ and $c_{14} = 9.0 \pm 0.4$ (quoted errors 1σ). The slope α is negative and inconsistent with 0 at 6.6σ. The previous studies of galaxy clusters ($M \gtrsim 10^{14} M_{\odot}$) with *Chandra* and *XMM* by Pointecouteau et al. (2005) and Vikhlinin et al. (2006) did not place strong constraints on α, and were quite consistent with $\alpha = 0$; i.e., it is the lower mass galaxy groups that require $\alpha < 0$ (see Gastaldello et al. 2006). Recent optical studies of the $c - M$ relation in the group-cluster regime (see §1) also do not place strong constraints on the slope and are very consistent with $\alpha = 0$. Our analysis, therefore, provides crucial evidence that c decreases with increasing M, as expected in CDM models (Navarro et al. 1997; Jing 2000; B01; D04; Macciò et al. 2006).

We compare the X-ray data to the ΛCDM1 model (with $\Omega_{\rm m} = 0.3$, $\sigma_8 = 0.9$, $n_s = 1$), the "concordance model" effectively representing the combined constraints from the first year of WMAP CMB data, supernovae, and galaxy surveys (e.g., Spergel et al. 2003). We judge the median $c - M$ relation of the ΛCDM1 model to be consistent with the empirical power-law fit provided the X-ray sample consists of the most relaxed, early forming systems, for which a systematic increase in the concentrations of $\approx 10\%$ is expected (Jing 2000; Wechsler et al. 2002; Macciò et al. 2006). We measure an intrinsic scatter in $\log_{10}(1+z)c$ of 0.102 ± 0.004 in excellent agreement with the prediction of CDM simulations for the most relaxed, early forming systems. The amount of scatter is a robust prediction of CDM variants and provides additional evidence that our sample comprises the most relaxed systems that are best suited for X-ray mass measurements requiring approximate hydrostatic equilibrium.

The X-ray $c - M$ relation places interesting constraints on σ_8. Within the context of the concordance model noted above, the $c - M$ relation requires $0.76 < \sigma_8 < 1.07$ (99% conf.). This confidence range is conservative as explained in §5.1.

Next we compare the X-ray data to the ΛCDM3 model (with $\Omega_{\rm m} = 0.26$, $\sigma_8 = 0.74$, $n_s = 0.95$) which updates the ΛCDM1 model using the analysis of the third year of WMAP data (Spergel et al. 2006). The X-ray $c - M$ relation rejects the ΛCDM3 model at more than the 99.99% confidence level. The primary reason for the poor performance of the ΛCDM3 model is the low value of σ_8, but the lower value of $\Omega_{\rm m}$ and the tilt of the power spectrum also contribute to the poor fit. For this comparison we have assumed a uniform bias for relaxed, early forming halos of $\approx 10\%$, as suggested by numerical simulations. This bias would have to be $\approx 50\%$ to bring the ΛCDM3 model into agreement with the X-ray data.

While the early-type galaxy and group-cluster mass halos ($\gtrsim 10^{13} M_{\odot}$) studied here apparently prefer slightly higher concentrations than predicted for typical halos in the concordance ΛCDM model, the opposite is true for late-type galaxies (e.g., Alam et al. 2002; van den Bosch et al. 2003; Dutton et al. 2005; Kuzio de Naray et al. 2006; Gnedin et al. 2006). This may indicate that a selection/formation-time bias operates across the galaxy type spectrum, with late-type galaxies inhabiting the low-concentration tail of the distribution.

Since D04 provide results of power-law fits to the $c - M$ relations of massive clusters formed in a variety of CDM models, including an open model and several dark energy models, we analyze separately the X-ray $c - M$ relation for the 22 systems in our sample with $M > 10^{14} M_{\odot}$. In this mass range we obtain c_{14} and $\alpha \approx 0$ values consistent with those inferred from previous *Chandra* and *XMM* studies in the cluster mass regime noted above (Pointecouteau et al. 2005; Vikhlinin et al. 2006). As also found for the entire sample, the $c - M$ relation of the high-mass subsample is consistent with the ΛCDM1 model and very inconsistent with the ΛCDM3 model.

However, an open model with $\Omega_{\rm m} \approx 0.3$ is ruled out ($> 99\%$ confidence) from joint consideration of only the X-ray $c - M$ relation and published constraints on σ_8 from the analysis of the abundances of galaxy clusters ($\sigma_8 > 0.70$, see §5.2). Since cluster abundance studies also find $\sigma_8 \approx 0.45$ if $\Omega_{\rm m} \approx 1$, using the X-ray $c - M$ data we find that we can also reject CDM models with $\Omega_{\rm m} \approx 1$ at a high significance level ($> 99.9\%$ confidence). Consequently, the combination of the X-ray $c - M$ relation and cluster abundances (and local constraints on the age of the universe) provides novel evidence for a flat, low-$\Omega_{\rm m}$ universe with dark energy using observations only in the local ($z \ll 1$) universe.

If the values of σ_8, $\Omega_{\rm m}$, and n_s of the ΛCDM3 model

are correct, agreement with the X-ray $c - M$ relation may be achieved by increasing the dark energy equation of state parameter w. We find that a quintessence model with $w \approx -0.8$ and $\sigma_8 = 0.82$ performs nearly as well as the ΛCDM1 model, and the larger value of w remains marginally consistent with supernova constraints (Astier et al. 2006).

Finally, we discuss key sources of systematic error associated with both the X-ray measurements and theoretical models that need to be addressed before the X-ray $c-M$ relation is suitable for precision cosmology. In particular, if the virial masses are systematically underestimated by $\sim 10\%$, as suggested by CDM simulations, then we estimate that c_{14} is increased by $\sim 5\%$, less than the $\approx 10\%$ increase expected for selecting relaxed, early forming systems. This level of systematic error does not change the conclusions of our present study (see §6.2), but it will be important for future studies of precision cosmology.

We thank A. Cooray for discussions and comments on the manuscript. D.A.B., P.J.H., and F.G. gratefully acknowledge partial support from NASA grants NNG04GE76G, issued through the Office of Space Sciences Long-Term Astrophysics program, and NAG5-13059, issued through the Office of Space Science Astrophysics Data Program. Partial support for this work was also provided by NASA through Chandra Award Numbers GO4-5139X and GO6-7118X issued by the Chandra X-ray Observatory Center, which is operated by the Smithsonian Astrophysical Observatory for and on behalf of NASA under contract NAS8-03060. We also are grateful for partial support from NASA-XMM grants, NAG5-13643, NAG5-13693, NNG04GL06G, and NNG05GL02G.

REFERENCES

Akritas, M. G. & Bershady, M. A. 1996, ApJ, 470, 706
Alam, S. M. K., Bullock, J. S., & Weinberg, D. H. 2002, ApJ, 572, 34
Allen, S. W., Ettori, S., & Fabian, A. C. 2001, MNRAS, 324, 877
Arnaud, M. 2005, astro-ph/0508159
Astier, P., Guy, J., Regnault, N., Pain, R., Aubourg, E., Balam, D., Basa, S., Carlberg, R. G., Fabbro, S., Fouchez, D., Hook, I. M., Howell, D. A., Lafoux, H., Neill, J. D., Palanque-Delabrouille, N., Perrett, K., Pritchet, C. J., Rich, J., Sullivan, M., Taillet, R., Aldering, G., Antilogus, P., Arsenijevic, V., Balland, C., Baumont, S., Bronder, J., Courtois, H., Ellis, R. S., Filiol, M., Gonçalves, A. C., Goobar, A., Guide, D., Hardin, D., Lusset, V., Lidman, C., McMahon, R., Mouchet, M., Mourao, A., Perlmutter, S., Ripoche, P., Tao, C., & Walton, N. 2006, A&A, 447, 31
Biviano, A. & Salucci, P. 2006, A&A, 452, 75
Blumenthal, G. R., Faber, S. M., Flores, R., & Primack, J. R. 1986, ApJ, 301, 27
Bridges, T., et, & al. 2006, MNRAS, in press (astro-ph/0608661)
Bryan, G. L. & Norman, M. L. 1998, ApJ, 495, 80
Bullock, J. S., Kolatt, T. S., Sigad, Y., Somerville, R. S., Kravtsov, A. V., Klypin, A. A., Primack, J. R., & Dekel, A. 2001, MNRAS, 321, 559
Buote, D. A. 2003, in The IGM/Galaxy Connection: The Distribution of Baryons at z=0, ASSL Conference Proceedings Vol. 281. Edited by Jessica L. Rosenberg and Mary E. Putman. ISBN: 1-4020-1289-6, Kluwer Academic Publishers, Dordrecht, 2003, p.87, 87
Buote, D. A. 2004, in IAU Symp. 220: Dark Matter in Galaxies, 149
Buote, D. A. & Tsai, J. C. 1995, ApJ, 439, 29
Chaboyer, B. 1998, Phys. Rep., 307, 23
Dolag, K., Bartelmann, M., Perrotta, F., Baccigalupi, C., Moscardini, L., Meneghetti, M., & Tormen, G. 2004, A&A, 416, 853
Dolag, K., Vazza, F., Brunetti, G., & Tormen, G. 2005, MNRAS, 364, 753
Dutton, A. A., Courteau, S., de Jong, R., & Carignan, C. 2005, ApJ, 619, 218
Dutton, A. A., et, & al. 2006, astro-ph/0604553
Eke, V. R., Navarro, J. F., & Steinmetz, M. 2001, ApJ, 554, 114
El-Zant, A. A., Hoffman, Y., Primack, J., Combes, F., & Shlosman, I. 2004, ApJ, 607, L75
Evrard, A. E., Metzler, C. A., & Navarro, J. F. 1996, ApJ, 469, 494
Gastaldello, F., et, & al. 2006, ApJ, submitted (astro-ph/0610134)
Gnedin, O. Y., Kravtsov, A. V., Klypin, A. A., & Nagai, D. 2004, ApJ, 616, 16
Gnedin, O. Y., Weinberg, D. H., Pizagno, J., Prada, F., & Rix, H.-W. 2006, ArXiv Astrophysics e-prints
Graham, A. W., et, & al. 2006, astro-ph/0608613
Hoekstra, H., Yee, H. K. C., & Gladders, M. D. 2002, ApJ, 577, 595
Hu, W. & Kravtsov, A. V. 2003, ApJ, 584, 702
Humphrey, P. J., Buote, D. A., Gastaldello, F., Zappacosta, L., Bullock, J. S., Brighenti, F., & Mathews, W. G. 2006, ApJ, 646, 899
Jarvis, M., Bernstein, G. M., Fischer, P., Smith, D., Jain, B., Tyson, J. A., & Wittman, D. 2003, AJ, 125, 1014
Jing, Y. P. 2000, ApJ, 535, 30
Kuhlen, M., Strigari, L. E., Zentner, A. R., Bullock, J. S., & Primack, J. R. 2005, MNRAS, 357, 387
Kuzio de Naray, R., McGaugh, S. S., de Blok, W. J. G., & Bosma, A. 2006, ApJS, 165, 461
Loeb, A. & Peebles, P. J. E. 2003, ApJ, 589, 29
Łokas, E. L., Wojtak, R., Gottlöber, S., Mamon, G. A., & Prada, F. 2006, MNRAS, 367, 1463
Macciò, A. V., et, & al. 2006, (astro-ph/0608157)
Mandelbaum, R., et, & al. 2006, astro-ph/0605476
Mathiesen, B., Evrard, A. E., & Mohr, J. J. 1999, ApJ, 520, L21
Nagai, D., et, & al. 2006, astro-ph/0609247
Navarro, J. F., Frenk, C. S., & White, S. D. M. 1997, ApJ, 490, 493
Navarro, J. F., Hayashi, E., Power, C., Jenkins, A. R., Frenk, C. S., White, S. D. M., Springel, V., Stadel, J., & Quinn, T. R. 2004, MNRAS, 349, 1039
Peebles, P. J. & Ratra, B. 2003, Reviews of Modern Physics, 75, 559
Pointecouteau, E., Arnaud, M., & Pratt, G. W. 2005, A&A, 435, 1
Primack, J. R. 2006, astro-ph/0609541
Rasia, E., Ettori, S., Moscardini, L., Mazzotta, P., Borgani, S., Dolag, K., Tormen, G., Cheng, L. M., & Diaferio, A. 2006, MNRAS, 369, 2013
Ratra, B. & Peebles, P. J. E. 1988, Phys. Rev. D, 37, 3406
Reiprich, T. H. 2006, A&A, 453, L39
Reiprich, T. H. & Böhringer, H. 2002, ApJ, 567, 716
Rines, K. & Diaferio, A. 2006, AJ, 132, 1275
Rines, K., et, & al. 2006, astro-ph/0606545
Sato, S., Akimoto, F., Furuzawa, A., Tawara, Y., Watanabe, M., & Kumai, Y. 2000, ApJ, 537, L73
Shaw, L. D., Weller, J., Ostriker, J. P., & Bode, P. 2006, ApJ, 646, 815
Spergel, D. N., et, & al. 2006, astro-ph/0603449
Spergel, D. N., Verde, L., Peiris, H. V., Komatsu, E., Nolta, M. R., Bennett, C. L., Halpern, M., Hinshaw, G., Jarosik, N., Kogut, A., Limon, M., Meyer, S. S., Page, L., Tucker, G. S., Weiland, J. L., Wollack, E., & Wright, E. L. 2003, ApJS, 148, 175
Stanek, R., Evrard, A. E., Böhringer, H., Schuecker, P., & Nord, B. 2006, ApJ, 648, 956
Tasitsiomi, A., Kravtsov, A. V., Gottlöber, S., & Klypin, A. A. 2004, ApJ, 607, 125
Tremaine, S., Gebhardt, K., Bender, R., Bower, G., Dressler, A., Faber, S. M., Filippenko, A. V., Green, R., Grillmair, C., Ho, L. C., Kormendy, J., Lauer, T. R., Magorrian, J., Pinkney, J., & Richstone, D. 2002, ApJ, 574, 740

Tsai, J. C., Katz, N., & Bertschinger, E. 1994, ApJ, 423, 553
van den Bosch, F. C., Mo, H. J., & Yang, X. 2003, MNRAS, 345, 923
Van Waerbeke, L., Mellier, Y., & Hoekstra, H. 2005, A&A, 429, 75
Vikhlinin, A., Kravtsov, A., Forman, W., Jones, C., Markevitch, M., Murray, S. S., & Van Speybroeck, L. 2006, ApJ, 640, 691
Wang, H. Y., et, & al. 2006, astro-ph/0608690
Wechsler, R. H., Bullock, J. S., Primack, J. R., Kravtsov, A. V., & Dekel, A. 2002, ApJ, 568, 52
Wu, X.-P. & Xue, Y.-J. 2000, ApJ, 529, L5
Zappacosta, L., et, & al. 2006, ApJ, in press (astro-ph/0602613)